

A Single-Phase Modelling for the Oxygen Uptake Rate in Excess Post-Exercise Oxygen Consumption

Maria Carolina Traina Gama

Universidade Estadual de Campinas - Unicamp

Claudio Alexandre Gobatto

Universidade Estadual de Campinas - Unicamp

Dimas Roberto Vollet (✉ dr.vollet@unesp.br)

Universidade Estadual Paulista - Unesp

Research Article

Keywords: dVO_2/dt , WEP, EPOC, physiological parameter, VO_2

Posted Date: February 16th, 2021

DOI: <https://doi.org/10.21203/rs.3.rs-220974/v1>

License: © ⓘ This work is licensed under a Creative Commons Attribution 4.0 International License.

[Read Full License](#)

1 A Single-Phase Modelling for the Oxygen Uptake Rate in Excess Post- 2 Exercise Oxygen Consumption

3

4 Maria Carolina Traina Gama¹, Claudio Alexandre Gobatto¹, Dimas
5 Roberto Vollet^{2,*}

6

7 ¹UNICAMP - Universidade Estadual de Campinas, Faculdade de Ciências Aplicadas,
8 Campus de Limeira, Limeira, SP, Brazil.

9 ²Unesp - Univ Estadual Paulista, IGCE, Departamento de Física, Campus de Rio
10 Claro, Rio Claro, SP, Brazil.

11 *corresponding author: e-mail: dr.vollet@unesp.br

12

13 Abstract

14 A two-parameters [a rate constant k and a factor f ($0 \leq f < 1$)] modelling, describing
15 satisfactorily the post-exercise oxygen uptake rate (V_{O_2}) as a function of the recovery
16 time (t), is presented. f controls the rate equation dV_{O_2}/dt , particularly at $t = 0$ where
17 $(dV_{O_2}/dt)_{t=0} \propto -k(1-f)$, a less abrupt decay than $(dV_{O_2}/dt)_{t=0} \propto -k$ expected from an
18 exponential. Fitting the model to a set of experimental V_{O_2} vs t data after a 3MT it was
19 found a set of values with f close to 0 and another with $f > 1/2$, with a narrow distribution
20 of values for the half-recovery time $\tau_{1/2} = (1/k) \ln[(2-f)/(1-f)]$ ($\langle \tau_{1/2} \rangle = 0.641$ min, $\sigma = 0.062$
21 min), very similar to that (T) found by fitting a model based on a logit transform
22 ($\langle T \rangle = 0.672$ min, $\sigma = 0.081$ min). The parameter f is a reliable index of the initial
23 acceleration of the oxygen uptake rate recovery (and likely of the heart rate recovery)
24 and, together with the half-recovery time $\tau_{1/2}$, may be a useful method in characterizing
25 and monitoring performs and exercise forms, very important in the physiology area.

26

27

28

29 Introduction

30 Three-minute all-out test (3MT) is a maximal effort evaluation protocol based
31 on the original model of critical power whose metabolic parameters of aerobic (EP) and
32 anaerobic (WEP) capacities are obtained through the mathematic analysis of a subject's
33 output power kinetics. The kinetics of output power of 3MT can determine important
34 parameters for training prescription such as some transition limits when it comes to
35 effort intensity¹. EP is the threshold that measures the transition from intense to severe
36 exercise and uses mainly oxidative metabolism^{1,2}, while WEP uses anaerobic sources
37 and is a finite amount of work carried until it runs out in severe intensity exercises³. The
38 post-exercise oxygen consumption (EPOC) after 3MT can provide important
39 information about the maximum effort performed by the individual.

40 Direct physiological parameters such as blood lactate concentration and oxygen
41 uptake measure the domains of intensity transition during exercise⁴. Researchers have
42 been using such physiological markers, collecting them right after exercise, to
43 determine the contribution of the aerobic and anaerobic energetic metabolisms⁵. EPOC
44 may physiologically represent the reestablishment of blood and muscular O₂ to ATP and
45 PCr resynthesis, as well as removing lactate from high intensity efforts⁶. Blood lactate
46 concentration and EPOC can reliably estimate the anaerobic capacity in 3MT⁷.

47 The oxygen uptake rate (V_{O_2}) recovery is conventionally assumed to proceed in
48 a biphasic manner, consisting of "fast" and "slow" components. The overall process has
49 been described by two simple exponentials and it has been acknowledged as the
50 standing model⁸⁻¹¹.

51 However, it has been argued¹² that application of two-exponential model to post-
52 exercise oxygen uptake rate and heart rate (HR) might be questionable, since metabolic
53 processes like lactate elimination could follow rather the mass action law, instead an
54 exponential decay. Besides that, the procedure by curve fitting to a first order
55 exponential decay in HR recovery, following max exercise, seem not to confirm that a
56 first order equation is the optimal model to establish the most appropriate exercise
57 protocol¹³. The time decaying obtained by this procedure varied unacceptably with
58 small changes in onset of monitoring and the residuals of the fitted curve were non-
59 random¹³.

60 Therefore, it is opportune to consider alternative models based on the mass
61 action law, for instance, to fit the experimental data. The mass action law requires that

62 the rate equation for V_{O_2} decaying takes into account two components: the residual
 63 “oxygen debt” ($V_{O_2} - V_{O_{2rest}}$) and the “oxygen debt” already paid ($V_{O_{2peak}} - V_{O_2}$), in a
 64 total net peak post-exercise uptake ($V_{O_{2peak}} - V_{O_{2rest}}$)¹². Stupnicki *et al.*¹², by applying a
 65 logit transform, $\log[X_i/(X_{peak}-X_i)]$, to the recorded variables X_i [post-exercise heart rate
 66 (HR) and V_{O_2}] and relating them to the decimal logarithm of the recovery time t ,
 67 obtained single-phase course of changes for both variables, rendering a linear
 68 relationship, which facilitated various comparisons. This logit–log transformation was
 69 also used with success to model horse post-exercise heart rate recovery¹⁴. However,
 70 Stupnicki *et al.*¹² did not give an analytical form to fit the data nor provided the rate
 71 equation for the V_{O_2} decaying.

72 In this work, the rate equation for the oxygen uptake rate decaying, dV_{O_2}/dt , is
 73 considered as being first-order on the fraction X of the residual “oxygen debt” to decay,
 74 and first-order on $(1-fX)$, a function of the fraction $(1-X)$ of the “oxygen debt” already
 75 paid, where f ($0 \leq f < 1$) is a factor introduced to control the recovery start. The
 76 approach provides an analytical form for the oxygen uptake rate as a recovery time
 77 function, without loss of generality, since, by setting $f = 0$, the model becomes just the
 78 standing mono-exponential one.

79 **Theoretical aspects**

80 **The f -single-phase modelling**

81 The rate equation, dV_{O_2}/dt , for the oxygen uptake rate (V_{O_2}) at the recovery
 82 instant t was assumed as being first-order on the fraction X of the residual “oxygen
 83 debt” to decay, $X = (V_{O_2} - V_{O_{2rest}})/(V_{O_{2peak}} - V_{O_{2rest}})$, where $V_{O_{2peak}}$ is oxygen uptake rate
 84 at $t = 0$ and $V_{O_{2rest}}$ the oxygen uptake rate at rest ($t \rightarrow \infty$), and first-order on $(1-fX)$, a
 85 function of the fraction $(1-X)$ of the “oxygen debt” already paid, $(1-X) = (V_{O_{2peak}} -$
 86 $V_{O_2})/(V_{O_{2peak}} - V_{O_{2rest}})$, where f , with the constraint $0 \leq f < 1$, is a factor introduced to
 87 control the recovery start. Since $dV_{O_2}/dt \propto dX/dt$, it follows

$$88 \quad \quad \quad dX/dt = -kX(1-fX) \quad , \quad (1)$$

89 where k (min^{-1}) is a rate constant. The parameter f controls the rate equation (equation
 90 (1)), particularly at $t = 0$ when $X = 1$, so

$$91 \quad \quad \quad (dX/dt)_{t=0} = -k(1-f) \quad . \quad (2)$$

92 The solution of equation (1), under the conditions $X = 1$ at $t = 0$ and $X = 0$ at $t \rightarrow$
 93 ∞ , is

$$94 \quad X = \exp(-kt) / \{1 - f[1 - \exp(-kt)]\} . \quad (3)$$

95 If $f = 0$, the decaying process is a simple exponential $X = \exp(-kt)$ and $(dX/dt)_{t=0} = -k$, a
 96 more abrupt decaying than $(dX/dt)_{t=0} = -k(1-f)$ when $f > 0$.

97 The half-recovery time ($\tau_{1/2}$), the time for X to decay to half of its initial value,
 98 can be evaluated from equation (3) as

$$99 \quad \tau_{1/2} = (1/k) \ln[(2-f)/(1-f)] . \quad (4)$$

100 Restoring the definition $X = (V_{O2} - V_{O2rest}) / (V_{O2peak} - V_{O2rest})$ in equation (3)
 101 yields

$$102 \quad V_{O2} = V_{O2rest} + (V_{O2peak} - V_{O2rest}) \exp(-kt) / \{1 - f[1 - \exp(-kt)]\} . \quad (5)$$

103 Equation (5), named here f -single-phase ($f1p$) model, can be fitted to the experimental
 104 V_{O2} vs t data to obtain the parameters k, f, V_{O2peak} and V_{O2rest} . Equivalently, equation (5)
 105 could be expressed in terms of the parameters k and $\tau_{1/2}$, since f can be solved from
 106 equation (4) as $f = [\exp(k\tau_{1/2}) - 2] / [\exp(k\tau_{1/2}) - 1]$, with the constraint $k\tau_{1/2} \geq \ln 2$.

107 Therefore, among the parameters k, f and $\tau_{1/2}$, only two of them are independent in the
 108 $f1p$ model.

109 The integral of equation (3) between $t = 0$ and t , $X_{integ}(t)$ (in min), when multiplied
 110 by the quantity $(V_{O2peak} - V_{O2rest})$, represents the total net volume of oxygen uptake up to
 111 the instant t , $VT_{O2net}(t)$, excluded the contribution of the rest component. $X_{integ}(t)$ can be
 112 evaluated by

$$113 \quad X_{integ}(t) = -(1/k)(1/f) \ln\{1 - f[1 - \exp(-kt)]\} , \quad (6)$$

114 so, the total integrated quantity, X_{integ} , between $t = 0$ and $t = \infty$, is

$$115 \quad X_{integ} = -(1/k)(1/f) \ln(1-f) = -\tau_{1/2}(1/f) \ln(1-f) / \ln[(2-f)/(1-f)] . \quad (7)$$

116 The constraint equation (4) has been used to write X_{integ} indistinctly in terms of k and f
 117 or $\tau_{1/2}$ and f in equation (7). If $f = 0$, equation (7) becomes $X_{\text{integ}} = 1/k = \tau_{1/2}/\ln 2$ just as in
 118 case of an exponential decay, since the limit of $(1/f)\ln[(1-f)]$ is -1 when $f \rightarrow 0$.

119 The total net volume of oxygen uptake up to complete recovery ($t = \infty$), $VT_{O2\text{net}}$,
 120 the so-called EPOC, is obtained by multiplying equation (7) by the quantity $(V_{O2\text{peak}} -$
 121 $V_{O2\text{rest}})$, or

$$122 \quad VT_{O2\text{net}} = (V_{O2\text{peak}} - V_{O2\text{rest}})X_{\text{integ}} \quad . \quad (8)$$

123 To better illustrate the effect of the parameter f on the experimental V_{O2} vs t
 124 curve, Figure 1 shows plots of equation (3) for several values of k (or f) for a fixed value
 125 of $\tau_{1/2} = \ln 2$. The inclination $(dX/dt)_{t=0} = -k(1-f)$ at $t=0$ is effectively less abrupt with
 126 increasing f (insert in Figure 1), and particularly less abrupt than an exponential decay
 127 where $(dX/dt)_{t=0} = -k$. The increase of the parameter f retards effectively the decaying of
 128 V_{O2} at the beginning of the recovery, however, the rate of decaying at $t = \tau_{1/2}$, $(dX/dt)_{\tau_{1/2}}$
 129 $= -(k/2)[1-f/2]$, becomes more abrupt with increasing f , as shown by the tangent dash
 130 lines plotted with slopes $(dX/dt)_{\tau_{1/2}}$ at $t = \tau_{1/2}$ in Figure 1 for several values of k (or f , since
 131 $\tau_{1/2} = \text{cte}$).

132 (insert Figure 1)

133

134 **About the logit transformation**

135 It is opportune to compare the present f 1p model with that could be inferred
 136 from a graphical procedure proposed by Stupnicki *et al.*¹². They applied a logit
 137 transformation, $\log[X_i/(X_{\text{peak}}-X_i)]$, to the net recorded variables X_i ($X_i = V_{O2} - V_{O2\text{rest}}$ and
 138 $X_{\text{peak}} = V_{O2\text{peak}} - V_{O2\text{rest}}$), and observed an unique regime of linear plot, with a negative
 139 slope $(-\alpha)$, in the whole domain of the logarithm of the recovery time t . Then, the
 140 relation $\log[X_i/(X_{\text{peak}}-X_i)] = -\alpha \log t + B$, where B is a constant, should be kept. By
 141 writing $B = \log T^\alpha$, where T is a characteristic time, it is concluded that $X_i =$
 142 $X_{\text{peak}}\{1/[(t/T)^\alpha + 1]\}$, or

$$143 \quad X = 1/[(t/T)^\alpha + 1] \quad , \quad (9)$$

144 to keep the same notation for the fraction $X = X_i / X_{\text{peak}} = (V_{O_2} - V_{O_{2\text{rest}}}) / (V_{O_{2\text{peak}}} - V_{O_{2\text{rest}}})$
 145 of the present work. So equation (9) could be written as

$$146 \quad V_{O_2} = V_{O_{2\text{rest}}} + (V_{O_{2\text{peak}}} - V_{O_{2\text{rest}}}) \{ 1 / [(t/T)^\alpha + 1] \} . \quad (10)$$

147 Equation (10), named here Stu model, could be fitted to the experimental V_{O_2} vs t data
 148 and the parameters α , T , $V_{O_{2\text{peak}}}$ and $V_{O_{2\text{rest}}}$ determined. T represents the half-recovery
 149 time, the time for X in equation (9) to decay to $1/2$, the same meaning of the parameter
 150 $\tau_{1/2}$ of the *f1p* model.

151 The rate equation that governs the decaying law of equation (9) is given by

$$152 \quad dX/dt = -(\alpha/T)X^{(1+1/\alpha)}(1-X)^{(1-1/\alpha)} , \quad (11)$$

153 being, therefore, of $(1+1/\alpha)$ -order on X and $(1-1/\alpha)$ -order on $(1-X)$. The overall order
 154 with respect to both, X and $(1-X)$, remains constant and equal to $(1-1/\alpha) + (1+1/\alpha) = 2$,
 155 independent on α . The parameter α should be ≥ 1 to avoid negative-order on $(1-X)$.
 156 With $\alpha > 1$, equation (11) gives always $(dX/dt)_{t=0} = 0$ at $t = 0$, which is different from
 157 $(dX/dt)_{t=0} = -k(1-f)$ of the *f1p* model. If $\alpha = 1$, the rate equation (11) would be a second-
 158 order on X and zero-order on $(1-X)$, and $(dX/dt)_{t=0} = -(1/T)$ at $t = 0$, as the unique
 159 exception.

160 **Material and methods**

161 Ten recreationally-trained male runners (24 ± 4 years; 80.3 ± 8.7 kg; 179 ± 5
 162 cm; $9.0 \pm 2.5\%$ body fat) participated in this study performing 3MT, after signing an
 163 informed consent form approved by the Human Research Ethics Committee of the
 164 University of Campinas (protocol CAAE: 61934516.5.0000.5404), in accordance with
 165 the Declaration of Helsinki.

166 3MT was carried out on a non-motorized treadmill (NMT) after a five-minute
 167 warm-up consisting in walking on a motorized treadmill (MT) at 6 km/h. Each
 168 participant ran on a NMT tethered to an adjustable-height pole by a steel cable attached
 169 to a load cell (CSL/ZL-250, MK Control and Instrumentation)¹⁵. Despite participants
 170 were constantly encouraged during the test, no information in regards of time was
 171 given. The test only was considered successful after 3 minutes of non-stoppable
 172 running. The mechanical output power generated by each subject during the 3MT test

173 was recorded and analyzed against time to find the aerobic capacity (EP) and anaerobic
174 work capacity (WEP) values of the power output graph².

175 The oxygen uptake and carbon dioxide production were measured by using a gas
176 analyzer (Cosmed Italy K4b²) that was calibrated after each session. The gas analyzer was
177 integrated to an online system of breath-by-breath data caption. The oxygen uptake rate (V_{O_2})
178 was measured as a function of the recovery time (t) up to about 10 min after the start of
179 the 3MT recovery. The models were fitted to the experimental V_{O_2} vs t data.

180 The fitting processes were carried out using a routine of least-squares method
181 based on the Levenberg-Marquardt algorithm. When was the case, the similarity
182 between the parameters given by different models was statistically tested for equal
183 means using One-Way ANOVA.

184 **Results**

185 Figure 2 shows the $f1p$ model fitting well the experimental V_{O_2} vs t . The fitted
186 parameters $V_{O_{2peak}}$, $V_{O_{2rest}}$, k , and f (or $\tau_{1/2}$) are shown in Table 1 ($f1p$ model) with the
187 respective standard errors. The data were organized in order of increasing f . When the
188 fitting process converged rapidly to the lower constraint value $f = 0$ (subjects 1 and 2 in
189 Table 1), f was set to 0 and k obtained by fitting, and $\tau_{1/2}$ evaluated through $\tau_{1/2} =$
190 $(1/k)\ln 2$. The mean value of $\tau_{1/2}$ was $\langle \tau_{1/2} \rangle = 0.641$ min with standard deviation $\sigma =$
191 0.062 min.

192 (insert Figure 2)

193 (insert Table 1)

194 Figure 3(a) shows the fitting of the Stu model to the experimental data of the
195 subject number 8, as an instance, in comparison with that of the $f1p$ model. The Stu
196 model fitted well all the present set of experimental data. Table 1 (Stu model) shows the
197 fitted parameters $V_{O_{2peak}}$, $V_{O_{2rest}}$, α , and T with the standard errors. Figure 3(b) shows
198 the adjusted R -square and the reduced sum of squares χ^2 obtained by fitting both the
199 models (Stu and $f1p$) to the experimental data. The mean value of the half-recovery time
200 T was $\langle T \rangle = 0.672$ min with standard deviation $\sigma = 0.081$ min. Figure 3(c) shows the
201 distribution of T and $\tau_{1/2}$ plotted as normal Gaussian distributions $F(\tau, \sigma) =$
202 $[1/(2\pi\sigma^2)^{1/2}]\exp[-((t-\tau)/\sigma)^2/2]$, using the mean values $\langle \tau_{1/2} \rangle$ and $\langle T \rangle$ with the respective
203 standard deviations (σ).

204 (insert Figure 3)

205 The standard biphasic two-exponential model, which can be cast as $V_{O_2} = V_{O_{2rest}}$
 206 $+ A_1 \exp(-t/\tau_1) + A_2 \exp(-t/\tau_2)$, where A_1 and A_2 are constants and τ_1 and τ_2 are the “fast”
 207 and the “slow” decaying constant times, respectively, was also fitted to the present
 208 experimental data. In order to minimize the parameters to be fitted, $V_{O_{2rest}}$ was fixed as
 209 the mean value of V_{O_2} in the last minute of recovery and the parameters A_1 , τ_1 , A_2 , and
 210 τ_2 were obtained by fitting. Table 1 (two-exponential model) shows the fitted
 211 parameters with the standard errors.

212 The constant times τ_1 and τ_2 were yet converted (in order to compare them with
 213 $\tau_{1/2}$) to the half-recovery times $\tau_{1/2}^{(1)}$ and $\tau_{1/2}^{(2)}$ by using $\tau_{1/2}^{(1)} = \tau_1 \ln 2$ and $\tau_{1/2}^{(2)} = \tau_2 \ln 2$.
 214 The mean values for $\tau_{1/2}^{(1)}$ and $\tau_{1/2}^{(2)}$ were $\langle \tau_{1/2}^{(1)} \rangle = 0.476$ min, with standard deviation
 215 $\sigma = 0.082$ min, and $\langle \tau_{1/2}^{(2)} \rangle = 3.94$ min, with standard deviation $\sigma = 1.91$ min.

216 Figure 4(a) shows the reduced residual sum of square (χ^2) and the adjusted R -
 217 square values obtained by fitting the standard biphasic two-exponential model and the
 218 $f1p$ model. Figure 4(b) shows normal Gaussian distributions $F(\tau, \sigma) =$
 219 $[1/(2\pi\sigma^2)^{1/2}] \exp[-((t-\tau)/\sigma)^2/2]$ plotted by using the mean value $\langle \tau_{1/2} \rangle$ ($f1p$ model) and
 220 the mean values $\langle \tau_{1/2}^{(1)} \rangle$ and $\langle \tau_{1/2}^{(2)} \rangle$ (standard biphasic model), with the respective
 221 standard deviations (σ).

222 (insert Figure 4)

223 Discussion

224 The values of f obtained by fitting the $f1p$ model define a group of individuals
 225 for which f was zero or lightly greater than zero [subjects 1 to 5, Table 1 ($f1p$ model)]
 226 and another for which $f > 1/2$ [subjects 6 to 10, Table 1 ($f1p$ model)]. $f > 0$ means that
 227 the rate equation at $t = 0$ [$(dX/dt)_{t=0} = -k(1 - f)$] is not so abrupt as in case of an
 228 exponential. This apparent bimodal distribution of f in this set of recreationally trained
 229 subjects may be characteristic of the individuals. Though this hypothesis could not be
 230 conclude by analyzing only this set of experimental data, it is clear that the present
 231 method opens large possibilities of investigation about exercises and individual
 232 performs through the parameter f .

233 Figure 5(a) shows that the values of $\tau_{1/2}$ obtained by the $f1p$ model, when
 234 analyzed as function of the parameter f , are randomly distributed along the horizontal
 235 line described by $\tau_{1/2} = \langle \tau_{1/2} \rangle = 0.641$ min (within the standard error $\sigma = 0.062$ min).

236 Indeed, the linear fitting of $\tau_{1/2}$ vs f in Figure 5(a) yields the fairly horizontal line given
 237 by $\tau_{1/2}(\text{min}) = 0.644 - 0.0066 \times f$. The constancy of $\tau_{1/2}$ may mean a characteristic of the
 238 exercise, opening other possibilities for further investigations. Under constant $\tau_{1/2}$, $k =$
 239 $(1/\tau_{1/2})\ln[(2-f)/(1-f)]$, which follows from equation (4), also fitted well to the
 240 experimental k vs f data [Figure 5(b)], yielding $\tau_{1/2} = 0.636$ min with standard error $\sigma =$
 241 0.022 min, in good agreement with $\langle \tau_{1/2} \rangle = 0.641$ min. In addition, X_{integ} (the second part
 242 of equation (7)) also fitted reasonably the experimental X_{integ} vs f data with constant $\tau_{1/2}$
 243 [Figure 5(c)], yielding $\tau_{1/2} = 0.646$ min with standard error $\sigma = 0.122$ min, also in good
 244 agreement with $\langle \tau_{1/2} \rangle$.

245 Figure 5(c) means that X_{integ} diminishes effectively with the increase of f , and so
 246 $VT_{O2\text{net}}$, except by the amplitude factor ($V_{O2\text{peak}} - V_{O2\text{rest}}$) in equation (8). By keeping
 247 higher the rate V_{O2} at the beginning of the recovery, which means higher f , the total
 248 integrated oxygen uptake is paid faster at the beginning of the process. This statement
 249 could be supported by computing the time τ_Q necessary for $X_{\text{integ}}(t)$ (equation (6)) to
 250 reach the fraction $[1 - \exp(-1)]$ (~63%) of the total X_{integ} (equation (7)). Evaluating
 251 equation (6) for $t = \tau_Q$ and dividing it to $[1 - \exp(-1)]X_{\text{integ}}$ yields

$$252 \quad \tau_Q = -\tau_{1/2} \ln \left\{ \frac{[(1-f)[1 - \exp(-1)] - (1-f)]/f}{\ln[(2-f)/(1-f)]} \right\} . \quad (12)$$

253 Equation (12) fitted reasonably well the experimental τ_Q vs f data with constant $t_{1/2}$
 254 [Figure 5(d)], yielding $\tau_{1/2} = 0.648$ min and standard error $\sigma = 0.135$ min, also in good
 255 agreement with $\langle \tau_{1/2} \rangle$.

256 The narrow distribution of $t_{1/2}$ in the f1p model ($\langle \tau_{1/2} \rangle = 0.641$ min, $\sigma = 0.062$
 257 min) is in agreement with that of T in the Stu model ($\langle T \rangle = 0.672$ min, $\sigma = 0.081$ min)
 258 [Figure 3(c)]. The distributions for $t_{1/2}$ and T were statistically tested for equal means
 259 using One-Way ANOVA yielding $F = 0.9223$ and $p = 0.3496$, which means that, at the
 260 0.05 level, the population means are not significantly different. However, the Stu model
 261 fitted a bit better the experimental V_{O2} vs t data [minor χ^2 and better R values in Figure
 262 3(b)]. Nevertheless, the integration of equation (9) from $t = 0$ up to $t = T_f$ (the
 263 experimental final time of measurement) to find X_{integ} by the Stu model (in analogy to
 264 equation (7) for the f1p model) gives a complex result: $T_f \text{Hypergeometric2F1}[1, 1/\alpha,$
 265 $1+1/\alpha, -(T_f/T)^\alpha]$, where $\text{Hypergeometric2F1}[1, 1/\alpha, 1+1/\alpha, -(T_f/T)^\alpha]$ is a complex
 266 function evaluable numerically only in advanced routines.

267 Figure 4(a) shows that χ^2 of the $f1p$ model were larger than those of the standard
 268 two-exponential model for individuals of the group with $f = 0$ or lightly greater than
 269 zero (subjects 1 to 5), while χ^2 were found minor than those of the standard model for
 270 the group of individuals with $f > 1/2$ (subjects 6 to 10). The same general aspects of
 271 quality apply to the R -square values from fitting both models (Figure 4(a)). This
 272 suggests that the standard two-exponential model could be not quite appropriated to fit
 273 experimental data that exhibit a not so high decaying of the rate V_{O_2} at the beginning of
 274 recovery, where the $f1p$ model previews a less abrupt decaying $[(dX/dt)_{t=0} = -k(1-f)]$
 275 when $f > 0$. This seems to be the case for the recovery following peak exercise, for
 276 which a first order equation is far to confirm to be the optimal model to establish the
 277 most appropriate exercise protocol¹³.

278 Apart from the fact that the standard two-exponential model to have more
 279 parameters to be fitted with respect to the single-phase models ($f1p$ or Stu), Figure 5(b)
 280 shows that the distribution of the “fast” half-recovery time $\tau_{1/2}^{(1)}$ was even larger
 281 ($\langle \tau_{1/2}^{(1)} \rangle = 0.476$ min, $\sigma = 0.082$ min) than $\tau_{1/2}$ of the $f1p$ model, and the distribution of
 282 the “slow” half-recovery time $\tau_{1/2}^{(2)}$ was too large ($\langle \tau_{1/2}^{(2)} \rangle = 3.94$ min, $\sigma = 1.91$ min),
 283 likely meaningless, even by fixing the rest parameter $V_{O_{2rest}}$ in the fitting process.

284 **Conclusions**

285 The present f -single-phase modelling is a simple and powerful method able to fit
 286 satisfactorily with only two parameters, a rate constant (k) and a factor f ($0 \leq f < 1$),
 287 experimental data of oxygen uptake rate in recovery process. The parameter f controls
 288 the rate equation dV_{O_2}/dt , particularly at $t = 0$ where $(dV_{O_2}/dt)_{t=0} \propto -k(1-f)$, a decay
 289 effectively less abrupt than $(dV_{O_2}/dt)_{t=0} \propto -k$, expected from an exponential. Fitting the
 290 modelling to a set of experimental V_{O_2} vs t data after a 3MT yielded a bimodal set of
 291 values for f (a set with $f = 0$ or close to zero and a set with $f > 1/2$) and a narrow
 292 distribution of values for the half-recovery time $\tau_{1/2} = (1/k)\ln[(2-f)/(1-f)]$, with a mean
 293 value $\langle \tau_{1/2} \rangle = 0.641$ min and standard deviation $\sigma = 0.062$ min. The distribution of $\tau_{1/2}$ was
 294 very similar to that found for the half-recovery time T ($\langle T \rangle = 0.672$ min, $\sigma = 0.081$ min)
 295 obtained by fitting a single-phase model, inferred from a graphical procedure based on a
 296 logit-log transformation. The parameter f is a reliable index of the initial acceleration of
 297 the oxygen uptake rate recovery (and likely of the heart rate recovery) and, together
 298 with the half-recovery time $\tau_{1/2}$, may be a useful method in characterizing and

299 monitoring performs and exercise forms.

300 **Author contributions**

301 The study was conceived and designed by C.A.G. and M.C.T.G. Supporting materials
302 and analysis tools were provided by C.A.G. Experimental data were collected and
303 processed by M.C.T.G. The single-phase 1fp model was conceived by D.R.V. All the
304 authors contributed writing the paper.

305

306 **Disclosure statement**

307 The authors declare that they have no competing interest.

308 **References**

- 309 1 Burnley, M., Doust, J.H. & Vanhatalo, A. A 3-min all-out test to determine peak
310 oxygen uptake and the maximal steady state. *Med. Sci. Sports Exerc.* **38**, 1995–2003.
311 <https://doi.org/10.1249/01.mss.0000232024.06114.a6> (2006).
- 312 2 Vanhatalo, A., Doust, J.H. & Burnley, M. Determination of critical power using a 3-
313 min all-out cycling test. *Med. Sci. Sports Exerc.* **39**, 548–555.
314 <https://doi.org/10.1249/mss.0b013e31802dd3e6> (2007).
- 315 3 Jones, A.M., Vanhatalo, A., Burnley, M., Morton, R.H. & Poole, D.C.. Critical power:
316 implications for the determination of VO₂ max and exercise tolerance. *Med. Sci. Sports*
317 *Exerc.* **42**, 1876–1890. <https://doi.org/10.1249/MSS.0b013e3181d9cf7f> (2010).
- 318 4 Vanhatalo, A. *et al.* The mechanistic bases of the power-time relationship: muscle
319 metabolic responses and relationships to muscle fibre type. *J. Physiol.* **594**, 4407–4423.
320 <https://physoc.onlinelibrary.wiley.com/doi/full/10.1113/JP271879> (2016).
- 321 5 Bertuzzi, R. *et al.* GEDAE-LaB: A free software to calculate the energy system
322 contributions during exercise. *PLoS ONE* **11**, e0145733.
323 <https://doi.org/10.1371/journal.pone.0145733> (2016).
- 324 6 Margaria, R., Edwards, H.T. & Dill, D.B. The possible mechanisms of contracting
325 and paying the oxygen debt and the role of lactic acid in muscular contraction. *Am. J.*
326 *Physiol.* **106**, 689–715. <https://doi.org/10.1152/ajplegacy.1933.106.3.689> (1933).

- 327 7 Zagatto, A.M.R. *et al.* 3-min all-out effort on cycle ergometer is valid to estimate the
328 anaerobic capacity by measurement of blood lactate and excess post-exercise oxygen
329 consumption. *Eur. J. Sport Sci.* **19**, 645–652.
330 <https://doi.org/10.1080/17461391.2018.1546338> (2018).
- 331 8 Ozyener, F., Rossiter, H.B., Ward, S.A. & Whipp, B.J. Influence of exercise intensity
332 on the on- and off-transient kinetics of pulmonary oxygen uptake in humans. *J. Physiol.*
333 **533**, 891–902. <https://doi.org/10.1111/j.1469-7793.2001.t01-1-00891.x> (2001).
- 334 9 Åstrand, P.O., Rodahl, K., Dahl, H.A. & Strømme, S.B. *Textbook of Work*
335 *Physiology*. (Human Kinetics, 2003).
- 336 10 Powers, S.K. & Howley, E.T. *Exercise Physiology*. (McGraw-Hill, 1996).
- 337 11 Short, K.R. & Sedlock, D.A. Excess postexercise oxygen consumption and recovery
338 rate in trained and untrained subjects. *J. Appl. Physiol.* **83**, 153–159.
339 <https://doi.org/10.1152/jappp.1997.83.1.153> (1997).
- 340 12 Stupnicki, R., Gabryś, T., Szmatlan-Gabryś, U. & Tomaszewski, P. Fitting a single-
341 phase model to the post-exercise changes in heart rate and oxygen uptake. *Physiol. Res.*
342 **59**, 357–362. https://www.biomed.cas.cz/physiolres/pdf/59/59_357.pdf (2010.)
- 343 13 Pierpont, G.L., Stolpman, D.R. & Gornick, C.C. Heart rate recovery post-exercise as
344 an index of parasympathetic activity. *J. Auton. Nerv. Syst.* **80**, 169–174.
345 <https://www.ncbi.nlm.nih.gov/pubmed/10785283> (2000).
- 346 14 Mata, F. Evaluation of horse fitness for exercise: the use of a Logit-Log function to
347 model horse postexercise heart rate recovery. *J. Equine Vet. Sci.* **34**, 1055–1058.
348 Online: <http://dx.doi.org/10.1016/j.jevs.2014.06.004> (2014).
- 349 15 Gama, M.C.T., dos Reis, I.G.M., Sousa, F.A.B. & Gobatto, C.A. The 3-min all-out
350 test is valid for determining critical power but not anaerobic work capacity in tethered
351 running. *PLoS ONE* **13**, e0192552. <http://dx.doi.org/10.1371/journal.pone.0192552>
352 (2018).
353

354 **Figure captions**

355 Figure 1. Plots illustrating the effect of varying k (or f) for a fixed value of the half-
 356 recovery time $\tau_{1/2} = \ln 2$, according to the f -single-phase model. The zoom inserted
 357 illustrates the inclination $(dX/dt)_{t=0} = -k(1-f)$ at $t = 0$ being less abrupt as f increases.
 358 The straight dash lines are tangent to the curves at $t = \tau_{1/2}$ so their inclinations $(dX/dt)_{t=\tau_{1/2}}$
 359 $= -(k/2)(1-f/2)$ are more abrupt as f (or equivalently k) increases.

360

361 Figure 2. Fitting the f -single-phase model (full lines) to the experimental data (points).
 362 The inserts show residuals of the fitting.

363

364 Figure 3. (a) Illustration of fitting the $f1p$ model and the Stu model to the experimental
 365 data of the subject 8. The inserts show residuals of the fittings. (b) Reduced residual
 366 sum of square (χ^2) and adjusted R -square (R) from fitting both models to the set of
 367 experimental data. (c) Normal Gaussian distributions of the half-recovery times $\tau_{1/2}$ and
 368 T projected using the mean values $\langle \tau_{1/2} \rangle$ and $\langle T \rangle$ and the respective standard deviations
 369 (σ).

370

371 Figure 4. (a) Reduced residual sum of square (χ^2) and adjusted R -square (R) from
 372 fitting the $f1p$ model and the standard biphasic two-exponential model to the
 373 experimental data. (b) Normal Gaussian distributions for the half-recovery times
 374 projected using the mean value $\langle \tau_{1/2} \rangle$ (for the $f1p$ model), and the mean values “fast”
 375 $\langle \tau_{1/2}^{(1)} \rangle$ and “slow” $\langle \tau_{1/2}^{(2)} \rangle$ (for the standard biphasic two-exponential model), with the
 376 respective standard deviations (σ).

377

378 Figure 5. Parameters and other quantities evaluated as a function of the parameter f for
 379 the $f1p$ model. (a) $\tau_{1/2}$: the linear fitting $\tau_{1/2} = 0.644 - 0.0066 \times f$ supporting that $\tau_{1/2}$ is
 380 practically a constant ($\tau_{1/2} = \langle \tau_{1/2} \rangle = 0.641$ min). (b) k : it was well fitted by $k =$
 381 $(1/\tau_{1/2}) \ln[(2-f)/(1-f)]$ (from equation (4)) with constant $\tau_{1/2} = 0.636$ min ($\sigma = 0.022$
 382 min). (c) X_{integ} : it was reasonably fitted by equation (7) with constant $\tau_{1/2} = 0.646$ min (σ
 383 $= 0.122$ min). (d) τ_Q : it was reasonably fitted by equation (12) with constant $\tau_{1/2} =$
 384 0.648 min ($\sigma = 0.135$ min).

385

386 Table 1. Fitted parameters for the *f*1p model, the Stu model, and the standing biphasic
 387 two-exponential model. Numbers between the brackets are standard errors estimated by
 388 the fitting.

Subject	<i>f</i> 1p model				
	V_{O2peak} (ml/min·kg)	V_{O2rest} (ml/min·kg)	k (min ⁻¹)	$\tau_{1/2}$ (min)	f
1	29.9 (0.8)	9.09 (0.19)	0.99 (0.06)	0.700 (0.045)	0
2	36.8 (0.5)	7.83 (0.09)	1.25 (0.04)	0.554 (0.015)	0
3	27.6 (0.8)	7.84 (0.14)	1.02 (0.16)	0.678 (0.057)	0.01 (0.22)
4	40.3 (0.9)	8.70 (0.16)	1.15 (0.12)	0.641 (0.039)	0.08 (0.19)
5	41.9 (1.2)	11.1 (0.2)	1.13 (0.11)	0.657 (0.052)	0.09 (0.20)
6	45.8 (1.2)	9.73 (0.19)	2.00 (0.22)	0.610 (0.037)	0.58 (0.10)
7	37.8 (0.7)	9.45 (0.12)	2.71 (0.23)	0.658 (0.024)	0.73 (0.06)
8	35.1 (0.9)	9.04 (0.15)	2.55 (0.26)	0.737 (0.037)	0.82 (0.04)
9	28.5 (1.0)	9.30 (0.17)	2.82 (0.40)	0.689 (0.057)	0.83 (0.03)
10	33.0 (1.2)	6.97 (0.19)	3.58 (0.49)	0.574 (0.038)	0.85 (0.02)
Subject	Stu model				
	V_{O2peak} (ml/min·kg)	V_{O2rest} (ml/min·kg)	α	T (min)	
1	32.0 (1.5)	7.08 (0.61)	1.08 (0.13)	0.622 (0.077)	
2	36.5 (0.6)	6.81 (0.16)	1.46 (0.06)	0.554 (0.022)	
3	25.9 (0.7)	7.50 (0.20)	1.84 (0.15)	0.775 (0.046)	
4	37.6 (0.8)	8.22 (0.21)	1.89 (0.11)	0.728 (0.031)	
5	39.0 (0.9)	10.7 (0.3)	1.95 (0.15)	0.759 (0.040)	
6	42.9 (0.9)	9.25 (0.23)	2.19 (0.15)	0.665 (0.028)	
7	35.8 (0.5)	9.21 (0.13)	2.43 (0.13)	0.597 (0.018)	
8	33.9 (0.7)	8.62 (0.18)	2.41 (0.17)	0.748 (0.030)	
9	27.8 (0.8)	9.00 (0.21)	2.39 (0.29)	0.696 (0.047)	
10	31.9 (1.0)	6.72 (0.20)	2.63 (0.25)	0.576 (0.030)	
Subject	two-exponential model				
	A_1 (ml/min·kg)	τ_1 (min)	A_2 (ml/min·kg)	τ_2 (min)	
1	16 (2)	0.47 (0.09)	8.3 (1.7)	2.9 (0.5)	
2	26 (1)	0.57 (0.04)	6.0 (1.0)	3.3 (0.4)	
3	18 (2)	0.85 (0.11)	2.2 (1.7)	4.4 (2.7)	
4	29 (5)	0.79 (0.12)	3.7 (5.5)	2.4 (1.8)	
5	29 (2)	0.77 (0.08)	4.6 (1.8)	5.1 (1.9)	
6	37 (2)	0.69 (0.06)	2.8 (1.9)	4.4 (2.8)	
7	31 (1)	0.65 (0.03)	0.8 (0.6)	9.9 (9.7)	
8	28 (1)	0.76 (0.06)	3.1 (0.9)	10.1 (4.8)	
9	20 (1)	0.74 (0.10)	2.3 (1.3)	7.1 (4.9)	
10	29 (1)	0.59 (0.06)	2.6 (1.1)	7.2 (4.1)	

389

Figures

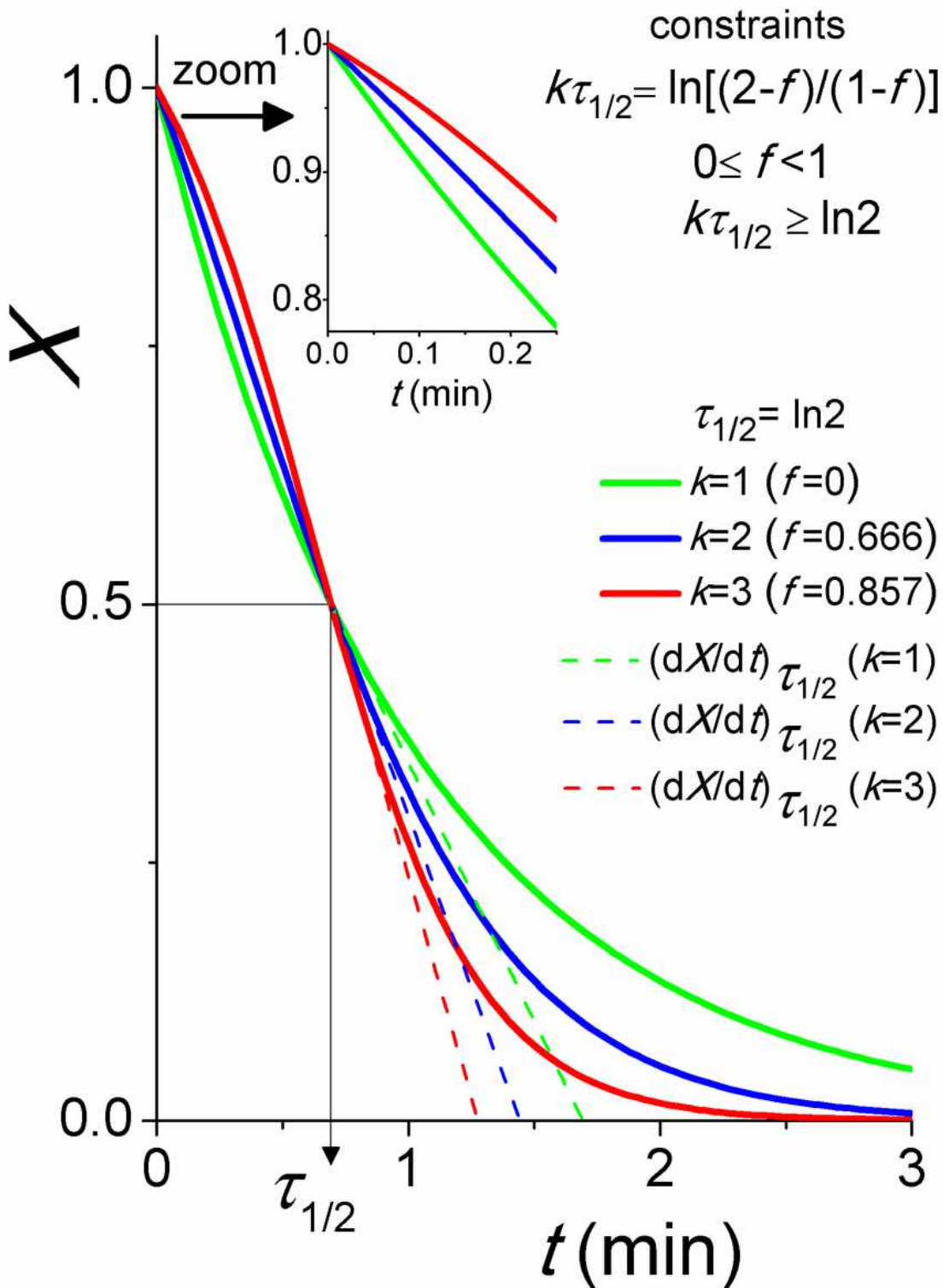


Figure 1

Plots illustrating the effect of varying k (or f) for a fixed value of the half-recovery time $t_{1/2} = \ln 2$, according to the f -single-phase model. The zoom inserted illustrates the inclination $(dX/dt)_{t=0} = -k(1-f)$ at

$t = 0$ being less abrupt as f increases. The straight dash lines are tangent to the curves at $t = t_{1/2}$ so their inclinations $(dX/dt)_{t=t_{1/2}} = -(k/2)(1-f/2)$ are more abrupt as f (or equivalently k) increases.

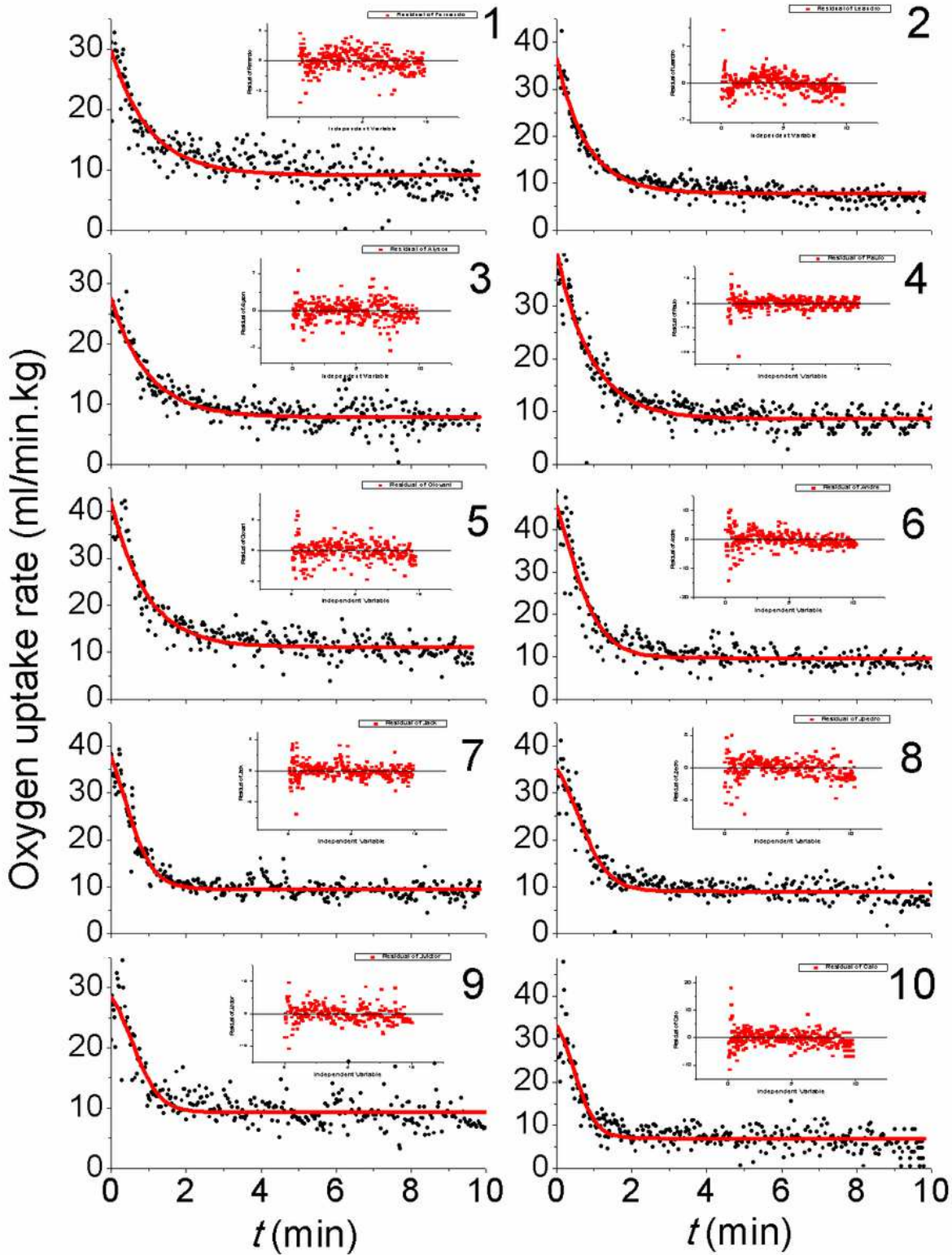


Figure 2

Fitting the f -single-phase model (full lines) to the experimental data (points). The inserts show residuals of the fitting.

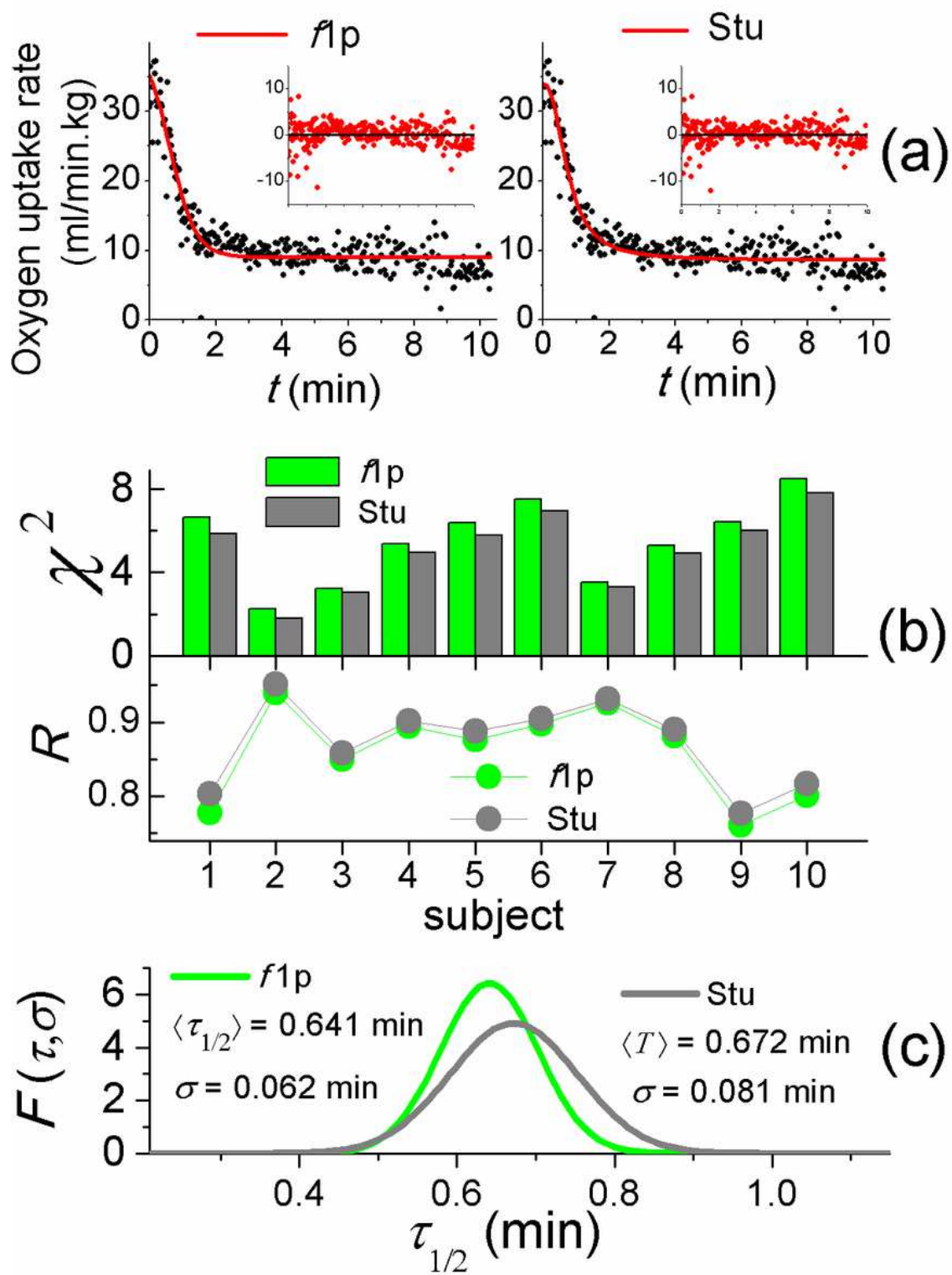


Figure 3

Please see the Manuscript Doc file for the complete figure caption.

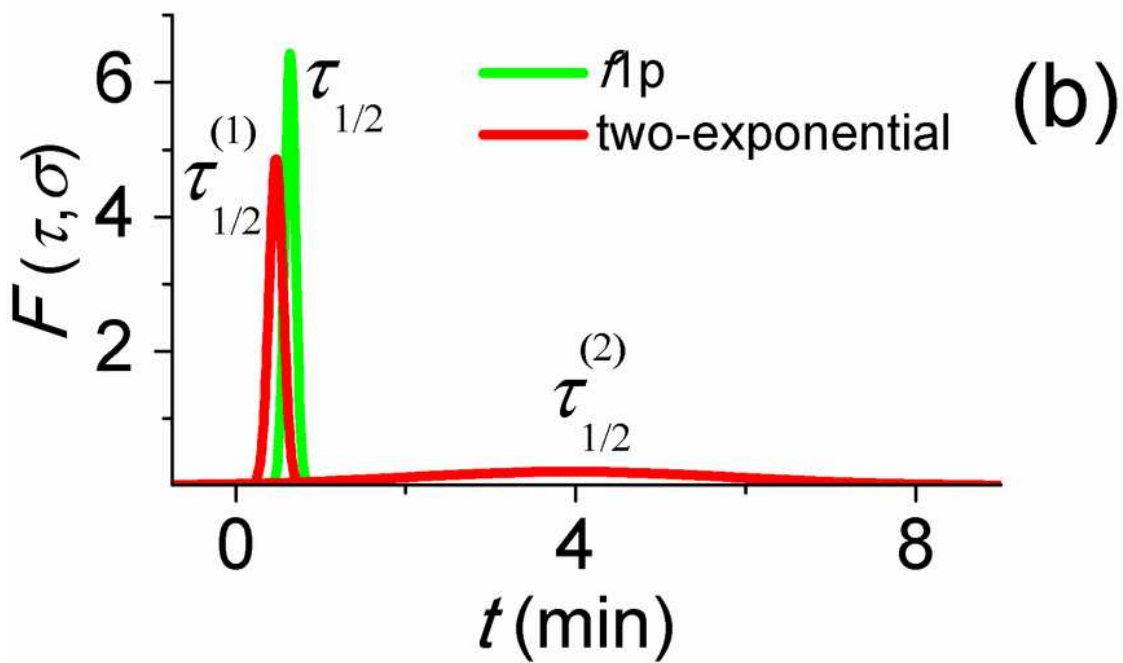
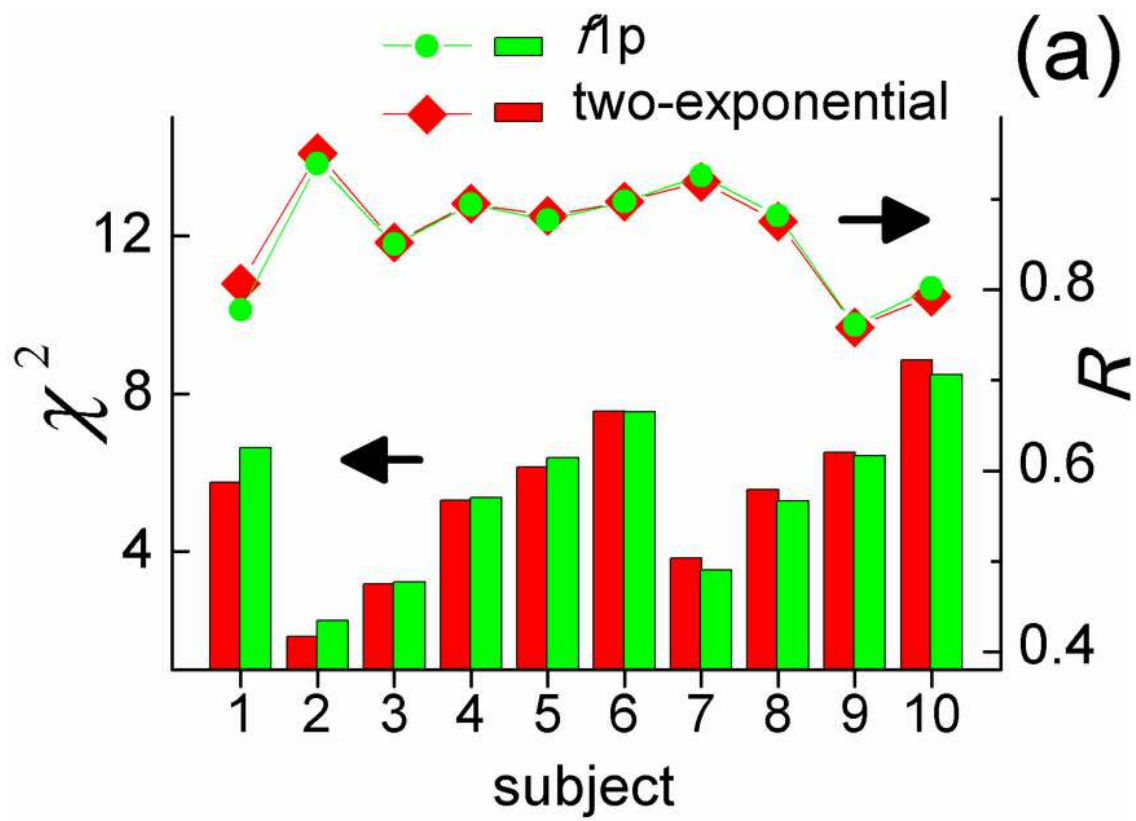


Figure 4

Please see the Manuscript Doc file for the complete figure caption.

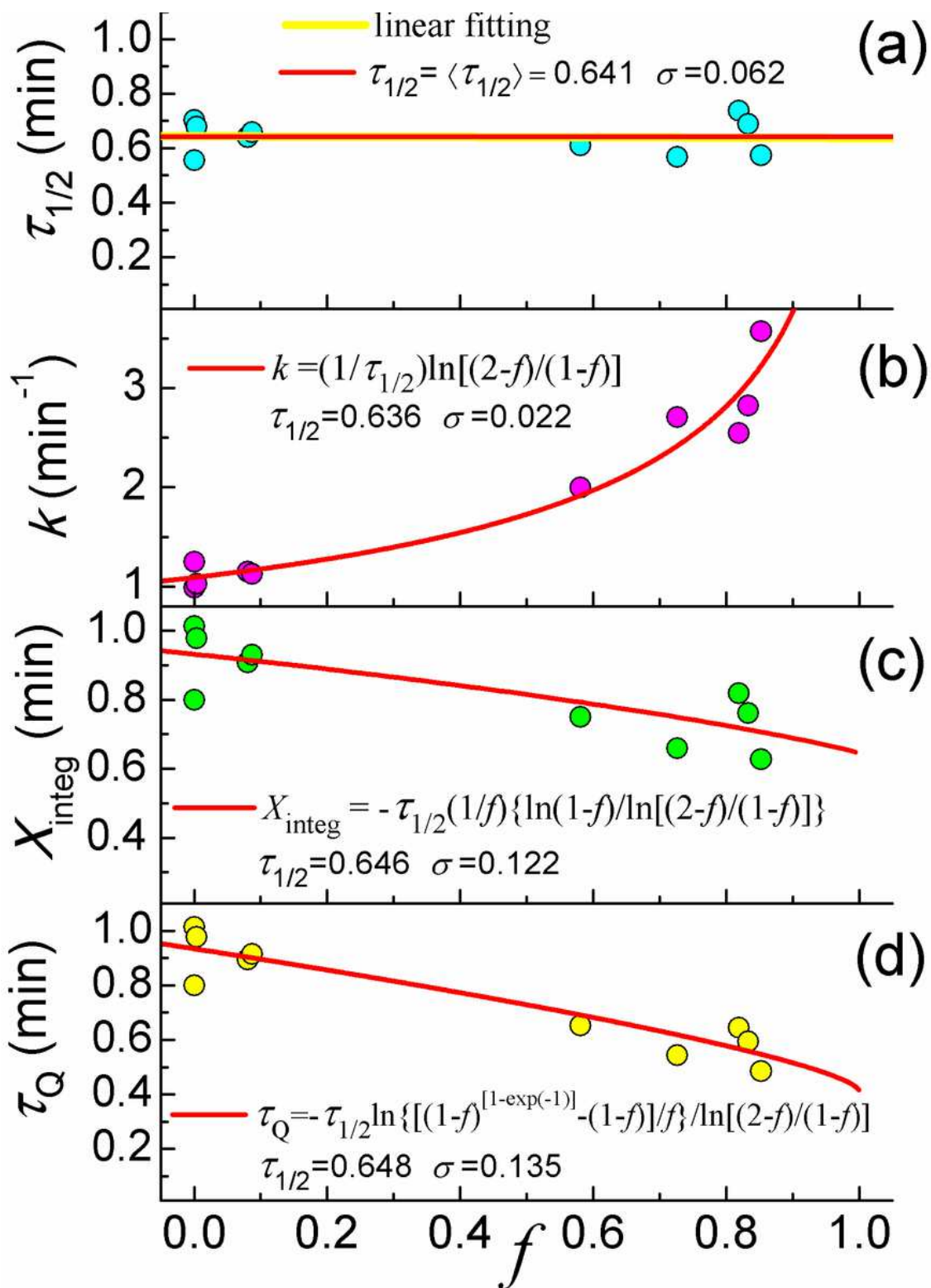


Figure 5

Please see the Manuscript Doc file for the complete figure caption.